

Pain matrix shift in the rat brain following persistent colonic inflammation revealed by voxel-based statistical analysis

Molecular Pain
Volume 15: 1–12
© The Author(s) 2019
Article reuse guidelines:
sagepub.com/journals-permissions
DOI: 10.1177/1744806919891327
journals.sagepub.com/home/mpx



Tianliang Huang^{1,2,3} , Takashi Okauchi¹, Di Hu¹, Mika Shigeta¹, Yuping Wu¹, Yasuhiro Wada⁴, Emi Hayashinaka⁴, Shenglan Wang³, Yoko Kogure³, Koichi Noguchi², Yasuyoshi Watanabe⁴, Yi Dai^{2,3}, and Yilong Cui¹

Abstract

Inflammatory bowel disease (IBD), mainly comprising Crohn's disease and ulcerative colitis, is characterized by chronic inflammation in the digestive tract. Approximately 60% of the patients experience abdominal pain during acute IBD episodes, which severely impairs their quality of life. Both peripheral and central mechanisms are thought to be involved in such abdominal pain in IBD. Although much attention has been paid to peripheral mechanisms of abdominal pain in IBD pathophysiology, the involvement of supraspinal mechanisms remains poorly understood. To address this issue, we investigated regional brain activity in response to colorectal distension in normal and IBD model rats using voxel-based statistical analysis of 2-deoxy-2-[18F]fluoro-D-glucose positron emission tomography imaging. The rat IBD model was generated by colorectal administration of 2,4,6-trinitrobenzene sulfonic acid, a chemical compound widely used to generate colitis. Tissue damage and inflammation were induced and dynamically changed with time after 2,4,6-trinitrobenzene sulfonic acid injection, while colorectal distension-induced visceromotor response showed corresponding temporal changes. We found that characteristic brain activations were observed in response to visceral innocuous and noxious colorectal distension and supraspinal nociception shared some physiological sensory pathway. Moreover, widespread brain regions were activated, and the functional coupling between the central medial thalamic nucleus and anterior cingulate cortex was enhanced after noxious colorectal distension in IBD model of rats. Increased brain activity in the anterior insular cortex and anterior cingulate cortex was positively correlated with noxious colorectal distension-induced pain severity in normal and IBD rats, respectively. These findings suggest that the pain matrix was shifted following persistent colonic inflammation, and thalamocortical sensitization in the pathway from the central medial thalamic nucleus to anterior cingulate cortex might be a central mechanism of the visceral hyperalgesia in IBD pathophysiology.

Keywords

Inflammatory bowel disease, persistent colonic inflammation, abdominal pain, pain matrix shifted, functional coupling

Date Received: 2 October 2019; revised: 30 October 2019; accepted: 4 November 2019

¹Laboratory for Biofunction Dynamics Imaging, RIKEN Center for Biosystems Dynamics Research, Kobe, Japan

²Department of Anatomy and Neuroscience, Hyogo College of Medicine, Nishinomiya, Japan

³Department of Pharmacy, School of Pharmacy, Hyogo University of Health Sciences, Kobe, Japan

⁴Laboratory for Pathophysiological and Health Science, RIKEN Center for Biosystems Dynamics Research, Kobe, Japan

Corresponding Authors:

Yilong Cui, Laboratory for Biofunction Dynamics Imaging, RIKEN Center for Biosystems Dynamics Research, 6-7-3 Minatojima minamimachi, Chuo-ku, Kobe, Hyogo 650-007, Japan.

Email: cuiyl@riken.jp

Yi Dai, Department of Pharmacy, School of Pharmacy, Hyogo University of Health Sciences, 1-3-6 Minatojima, Chuo-ku, Kobe, Hyogo 650-8530, Japan.

Email: ydai@huhs.ac.jp



Introduction

Inflammatory bowel disease (IBD) is a chronic inflammatory disorder characterized by swollen and damaged tissues in the digestive tract and mainly comprises Crohn's disease (CD) and ulcerative colitis (UC). Patients with IBD often complain for symptoms such as diarrhea, blood stool, abdominal pain, cramping, and so on.¹ Abdominal pain is a common and most disturbing symptom arising from the inflamed part of the digestive tract, even during daily physiological events, such as the defecation, exhaustion, and food ingestion, thus severely impairing the patients' quality of life.² Both peripheral and central mechanisms are known to be involved in such abdominal pain in IBD. In the peripheral tissue, inflammatory mediators released from the damaged tissue were reported to induce primary afferent nerve sensitization, thus decreasing the activation threshold of afferent nerve terminals, such as those containing adenosine triphosphate, serotonin, prostaglandin, bradykinin, and histamine.³ The upregulated expression level of transmembrane ion channels (sodium channels Nav 1.8 and 1.9),⁴ transient receptor potential family (TRPV1, TRPV4, and TRPA1), acid-sensing ion channels,^{5,6} and nerve growth factor was also proposed to be involved in peripheral visceral hypersensitivity.⁷ Despite the growing body of evidence has demonstrated that the sensitization of spinal cord dorsal horn neurons critically contributes to central visceral hypersensitivity in IBD pathophysiology,⁸ the involvement of higher order brain regions was still not fully understood.

Recently, few pioneering neuroimaging studies have reported that several higher order brain regions may contribute to abdominal pain in IBD. For example, in their functional magnetic resonance imaging (fMRI) clinical study, Bernstein et al.⁹ found that brain activity increased in the anterior cingulate cortex (ACC) and got suppressed in the somatosensory cortex (S1) in response to noxious visceral stimulation during the symptomatic remission period in patients with IBD (four with CD and two with UC). In contrast, using positron emission tomography (PET), Mayer et al.¹⁰ showed that several brain regions, such as lateral frontal regions and the dorsal pons/periaqueductal gray, were activated by noxious colorectal distension (CRD) in patients with quiescent UC. However, because of the limited number of studies and various criteria for patient recruitment, higher order brain regions contributing to abdominal pain in IBD remain incompletely understood.

With advances in imaging technologies, noninvasive neuroimaging methods, such as fMRI and PET, are increasingly used for obtaining a global overview of neural activity in rodent brain.^{11,12} Recently, we developed a small-animal neuroimaging method combining 2-

deoxy-2-[18F]fluoro-D-glucose (FDG) PET imaging with statistical parametric mapping analysis and demonstrated that the high-order trigeminal nociceptive pathway is activated by migraine attacks in an experimental model of migraine in rats.¹³ Although the spatiotemporal resolution of fMRI is superior to that of PET, FDG-PET has an advantage in examining the rat brain activity as FDG is taken up by active brain regions and remains within the system for at least an hour. Therefore, FDG-PET imaging is a useful tool for investigating brain activity, free from anesthesia. Using the FDG-PET imaging and subsequent voxel-based statistical analysis, we investigated the supraspinal brain activity induced by innocuous and noxious CRD in the normal and 2,4,6-trinitrobenzene sulfonic acid (TNBS)-induced IBD model rats.

Materials and methods

All experimental protocols were approved by the Institutional Animal Care and Use Committee of RIKEN, Kobe Branch, and all experiments were performed in accordance with the Principles of Laboratory Animal Care (National Institutes of Health Publication No. 85-23, revised 1985).

Animal preparation for generation of IBD model in rats

Male Sprague-Dawley rats (SLC, Hamamatsu, Shizuoka, Japan) weighing approximately 240 g were used. Rats were housed in a 12-h light/dark cycle at 22°C ± 1°C and received food and water ad libitum. The experimental IBD model was induced by local administration of TNBS (Nacalai Tesque, Kyoto, Japan) into the colon, as previously reported.^{6,14} Briefly, rats were fasted for 24 h prior to TNBS administration, and 50 mg/kg of TNBS dissolved in 50% ethanol in a volume of 1.25 mL/kg was administered into the colon, 6 cm proximal to the anus, using a syringe needle, under 1.5% isoflurane anesthesia. Then, the rats were maintained in a head-down position for 30 min. Rats in the sham group were given an enema of the same volume containing 0.9% saline. A body weight loss more than 15% of total body weight and serious bloody stool in the TNBS-injected rats was defined as a humane end point.

Implantation of the electrodes

For recording abdominal muscle contraction, three Teflon-insulated flexible wires (AS 633; Cooner Wire, Chatsworth, CA, USA) were chronically implanted into the external oblique muscle of rats 1 week before the experiment. Briefly, rats were anesthetized under a mixture of 1.5% isoflurane and oxygen/nitrous oxide

(3:7) and kept on a heating blanket during surgery to maintain body temperature. Two flexible wires were sutured into the right external oblique muscle with an approximate 1.5-cm distance, and another flexible wire was sutured into the opposite side of the external oblique muscle. All electrode leads were threaded through the subcutaneous tissue and externalized at the back of the rats and anchored to the back skin with a suture. Following surgery, rats were allowed to recover for five-days before the experiment and adequately acclimated to a cylindrical box (diameter: 6 cm, length: 16 cm) and insertion of an uninflated colorectal balloon for 15 min per two days.

Visceromotor response to CRD

After a few days of acclimation, visceromotor response (VMR) to CRD was measured to evaluate the severity of abdominal pain in conscious rats, which were adequately accustomed and remained quiet even during CRD, as previously reported.¹⁵ Briefly, electromyographic (EMG) signals from the external oblique muscle were amplified and filtered (0.3–1000 Hz) using a biological amplifier (Bio Amp; ADInstruments, Australia) and recorded by a PowerLab system (PowerLab 8/35, Chart, ADInstruments, Australia). Before CRD, a balloon (length: 4 cm) attached to a catheter was inserted intra-anally 6 cm proximal to the anus, and the balloon catheter was fixed on the rat's tail with tape. Few minutes after the balloon insertion, rats were left conscious in the cylindrical box (diameter: 6 cm, length: 16 cm) for 5 min. The CRD was performed three times by uniformly inflating up (260 mL/h) to 60 mmHg in a period of 10 s with an interval of 5 min. VMR magnitude was quantified as the maximal value of the area under the curve (AUC) of EMG signals for 10 s at 60 mmHg and normalized as ratio to the baseline before the CRD. VMR threshold was defined as the pressure in which the EMG-AUC/s increased to five times more than the value at baseline (10 s) before the CRD.

PET scanning

All PET scans were performed using a microPET Focus220 (Siemens Co., Ltd, Knoxville, TN, USA), with a spatial resolution of 1.4 mm in full width at half maximum (FWHM) at the center of the field of view, as previously reported.¹² Briefly, all rats received tail vein cannulation under 1.5% isoflurane and oxygen/nitrous oxide (3:7) prior to PET scanning. After more than 1 h of recovery from anesthesia, they were placed in a cylindrical box (diameter: 6 cm, length: 16 cm), and a balloon (length: 4 cm) attached to a catheter was inserted 6 cm into the distal colon from the anus. The catheter was fixed to the tail with tape. Rats were then left conscious

in the cylindrical box for 15 min. EMG signals were recorded using a data acquisition system and software (PowerLab 8/35, Chart, ADInstruments, Australia) during the CRD. Then, rats received an intravenous injection of 18F-FDG (ca. 70–75 MBq/0.4 mL). Immediately after the injection of 18F-FDG, CRD was performed 12 times by rapidly inflating up to 25 and 60 mmHg in a period of 10 s with an interval of 30 s in the normal (25 mmHg), normal (60 mmHg), and TNBS (60 mmHg) groups. A balloon was inserted in the normal (0 mmHg) group but without inflation. VMR magnitude was quantified as the AUC of EMG for the stimulation period and normalized as ratio to the baseline value before the CRD. Forty-five minutes after 18F-FDG injection, rats were anesthetized with 1.5% isoflurane and placed in the gantry of a PET scanner. During the scan, body temperature was maintained at about 37°C using a heating blanket connected with a thermo-controller, and a thermocouple probe was inserted into the rectum to monitor rectal temperature for feedback control of body temperature. Fifty-five minutes after 18F-FDG injection, a 30-min emission scan was performed, and data were collected in the three-dimensional list mode, sorted into a single sinogram, and reconstructed by a statistical maximum a posteriori probability algorithm (MAP) for image coregistration, or by standard two-dimensional-filtered back projection (FBP) algorithm for quantitative evaluation.

Image analysis

Voxel-based statistical analysis was performed according to the method described in the previous reports.¹² Briefly, individual MAP-reconstructed images were coregistered to an FDG image template using a mutual information algorithm with Powell's convergence optimization method supported by PMOD software package (version 3.6, PMOD Technologies, Ltd, Zurich, Switzerland). Then, we transformed the FDG template into the space of a magnetic resonance imaging reference template, which was placed in Paxinos and Watson stereotactic space. The transformation parameters obtained from individual MAP-reconstructed FDG images were applied to each FBP-reconstructed FDG image. The voxel size of the template was scaled by a factor of 10 to use the default parameter setting in SPM software (Wellcome Department of Imaging Neuroscience, London, UK). Then, the voxel size was resampled at $1.2 \times 1.2 \times 1.2$ mm. Finally, each FBP image was spatially smoothed using an isotropic Gaussian kernel (6-mm FWHM) for enhancement of the statistical power.

Voxel-based statistical analysis was performed using SPM 8 software (Wellcome Department of Imaging Neuroscience). Global uptake differences of FDG were normalized to the whole-brain uptake. A two-sample

t test was used for estimating the statistical differences between groups. The statistical threshold was set at $p < 0.005$ (uncorrected) with an extent threshold of 200 contiguous voxels.

Histological analysis

The rats were deeply anesthetized with 5% isoflurane and oxygen/nitrous oxide (3:7). Colon samples (5 cm above the anus, 3 cm in length) were removed and cut into sections of 1.5 cm and were fixed in 4% buffered paraformaldehyde for 24 h. The tissue was then transferred to a 30% sucrose solution for 72 h and stored at 4°C until use. It was then sectioned at 5 μm, and sections were stained with hematoxylin and eosin, according to our previous study.¹⁶

Data analysis

Statistical analysis of the behavioral tests was performed using SPSS 18.0 (SPSS Inc., Chicago, IL, USA). Differences in VMR magnitude obtained from normal (0, 25, and 60 mmHg) and TNBS (60 mmHg) groups in response to CRD were tested by one-way analysis of variance (ANOVA) followed by Tukey multiple-comparison test. Two-way ANOVA followed by Bonferroni multiple-comparison test was used to test the statistical differences in VMR magnitude and VMR threshold between sham- and TNBS-injected rats over time. Pearson's test was used for correlation analysis (VMR magnitude vs. FDG uptake in anterior insular cortex [aINS] and ACC, and FDG uptake in the central medial thalamic nucleus [CMT] vs. ACC). Fisher's Z-transformation test was applied to assess the significance of the difference between two correlation coefficients. Differences were considered statistically significant for $p < 0.05$. All results are expressed as the mean ± standard error of the mean.

Results

TNBS-induced colonic inflammation and visceral hyperalgesia in rats

As reported previously, several representative symptoms, such as bloody stool, poor coat quality, and reduced mobility, quickly developed after TNBS injection.¹⁷ Severe colonic damage and inflammation were observed in TNBS-injected rats, which persisted up to day 8 (Figure 1(a)). To further evaluate the abdominal pain severity in sham- and TNBS-induced IBD model rats, we recorded and analyzed EMG activity that was usually used for objective assessment of abdominal pain severity^{6,18} from the external oblique muscle under conscious conditions. Specifically, the VMR threshold, that

is, a CRD pressure inducing increment of more than five times of baseline EMG activity, was 39.5 ± 3.48 mmHg (Figure 1(b)), and the mean VMR magnitude, that is, the integrated EMG activity during stable CRD pressure at 60 mmHg, was 9.88 ± 2.65 (Figure 1(c)). In TNBS-injected rats, the CRD-induced VMR threshold and magnitude were dynamically changed. The VMR threshold significantly decreased during the period of inflammation with a peak at two days after TNBS injection (Figure 1(b)). The VMR magnitude apparently significant increased at two days after TNBS injection (Figure 1(c)).

High-order visceral nociceptive pathway shared visceral sensory circuit in the brain

In order to investigate whether the high-order visceral nociceptive pathway overlaps with physiological visceral sensory transmission circuit, we compared the regional brain activity induced by innocuous and noxious CRD in normal rats using FDG-PET scan and subsequent voxel-based statistical analysis. The innocuous and noxious CRD were performed at distention pressure below (25 mmHg) and above (60 mmHg) the VMR threshold (Figure 1(b)), respectively. Regional brain activity in each group was assessed by comparing the regional FDG uptake to that of the normal group in which rats received balloon insertion but not CRD (0 mmHg). As shown in Figure 2(a) and (b), the VMR magnitude was significantly increased in response to noxious CRD (60 mmHg), whereas no obvious changes in VMR magnitude were observed after the innocuous CRD (25 mmHg). Voxel-based statistical analysis showed characteristic activation pattern in each group (Figure 3). Regional brain activity in noxious CRD (Table 1) involved a wider brain area than that in innocuous CRD (Table 2), such as the aINS, anterior amygdaloid area (AA), parabrachial nucleus (PBN), and so on. Meanwhile, regional brain activity in several brain regions apparently contributed to both innocuous and noxious CRD, including the primary motor cortex (M1), the secondary somatosensory cortex (S2), CMT, and locus coeruleus (LC). These results indicate that high-order visceral nociception shares some physiological sensory transmission pathway.

The aINS has been usually reported to be involved in acute visceral noxious stimulation in human and rats.^{11,19} To further identify the functional role of the aINS in response to noxious CRD in physiological condition, we analyzed the correlation between FDG uptake in the aINS and VMR magnitude induced by 60-mmHg CRD in normal rats. As shown in Figure 4, FDG uptake in the aINS was positively correlated with the VMR magnitude ($n = 11$, $r = 0.72$, $p = 0.012$), indicating that

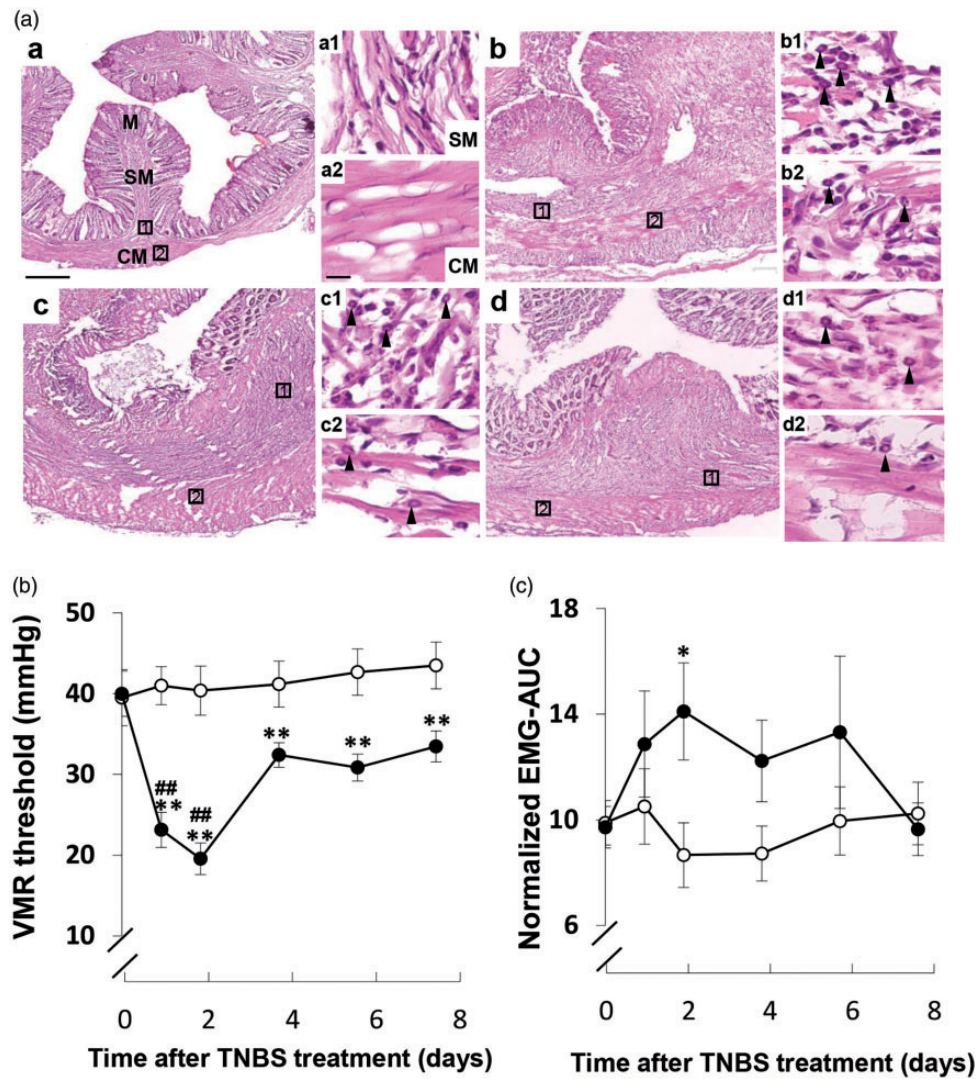


Figure 1. Changes in colonic inflammation and VMR in response to colorectal distension (CRD) in sham- and TNBS-injected rats. (a) Hematoxylin and eosin staining before (a) and two (b), four (c), and eight (d) days after TNBS injection ($n = 3$). Tissue damage in the M and SM and inflammatory cell infiltration in the SM and CM layer were observed at two, four, and eight days after TNBS injection. Rectangles in (a) to (d) indicate enlarged areas in high-magnification photomicrographs (a1–a2, b1–b2, c1–c2, and d1–d2) on the right side of each figure. Scale bars in (a) and (a2) indicate $500 \mu\text{m}$ and $50 \mu\text{m}$, respectively. Arrowheads in high-magnification photomicrographs indicate representative inflammatory cells. (b) Temporal changes in VMR threshold in the sham- (open circle, $n = 10$) and TNBS-injected (closed circle, $n = 13$) rats. (c) Temporal changes in VMR magnitude in response to noxious CRD at a pressure of 60 mmHg in the sham- ($n = 10$) and TNBS-injected ($n = 13$) rats. * $p < 0.05$ and ** $p < 0.01$ versus sham, ### $p < 0.01$ versus pre-TNBS injection; two-way ANOVA followed by Bonferroni multiple-comparison test. Each value represents the mean \pm standard error of the mean. CM: circuit muscle; EMG-AUC: the maximal value of the area under the curve of electromyographic signals; M: mucosa; SM: submucosa; TNBS: 2,4,6-trinitrobenzene sulfonic acid; VMR: visceromotor response.

regional brain activity in the aINS encodes visceral pain severity in normal rats.

Pain matrix in the brain shifted following persistent colonic inflammation

To further investigate whether and how the noxious CRD induced brain activity change in IBD model of rats, we assessed the brain regional FDG uptake in the

rats two days after TNBS injection, where the rats received noxious CRD at a distention pressure of 60 mmHg . As shown in Figure 2(a) and (b), the VMR magnitude was drastically increased in TNBS-injected rats as compared with noxious CRD with same distention pressure (60 mmHg) in normal rats, suggesting the visceral hyperalgesia had been developed in the TNBS-injected rats. In these rats, strong activation was observed in response to noxious CRD in

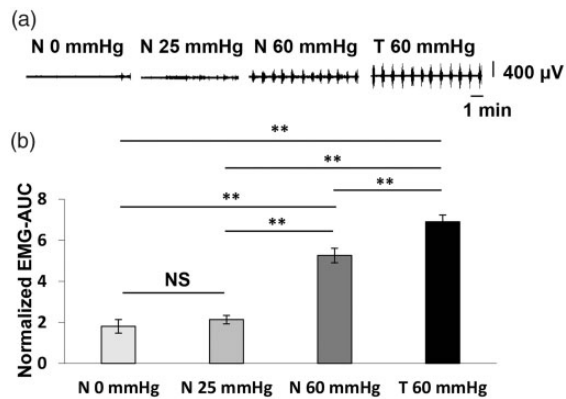


Figure 2. Visceromotor response (VMR) induced by different colorectal distension (CRD) pressures after 2-deoxy-2- ^{18}F fluoro-D-glucose (FDG) injection. (a) Representative EMG activity recorded from the external oblique muscle and corresponding CRD pressure in normal (N 0 mmHg), innocuous CRD (N 25 mmHg) and noxious CRD (N 60 mmHg) in normal rats, and noxious CRD (T 60 mmHg) in 2,4,6-trinitrobenzene sulfonic acid (TNBS)-injected rats after FDG injection. (b) VMR magnitude in response to different CRD pressures in normal (N 0 mmHg, $n = 13$), innocuous CRD (N 25 mmHg, $n = 9$) and noxious CRD (N 60 mmHg, $n = 11$) in normal rats, and noxious CRD (T 60 mmHg, $n = 13$) in TNBS-injected rats. Each value represents the mean \pm standard error of the mean. $**p < 0.01$; one-way ANOVA followed by Tukey multiple-comparison test. EMG-AUC: the maximal value of the area under the curve of electromyographic signals; NS: no significance.

widespread brain regions, such as the secondary motor cortex (M2), the cingulate cortex (ACC, midcingulate cortex, and posterior cingulate cortex), septal nucleus, and hippocampus (Figure 3; Table 3). Interestingly, increased brain activity in the M1 and S2 was also observed in these TNBS-injected rats (Table 3), indicating that the nociceptive pathway after colonic inflammation partially shared the physiological sensory transmission circuit. In contrast, activation of the aINS and AA and suppression of the CMT and PBN could not be observed in the TNBS-injected rats as observed with noxious CRD in normal rats, suggesting that the pain matrix shifted following the persistent colonic inflammation.

Recently, increased activity in the ACC has been reported after noxious CRD stimulation in healthy volunteers and patients with chronic visceral pain.^{10,20} To identify the functional role of the ACC in response to noxious CRD in IBD pathophysiology, we performed correlation analysis between the FDG uptake in the ACC and VMR magnitude induced by noxious CRD in TNBS-injected rats. As shown in Figure 5, the brain activity in the ACC was positively correlated with the VMR magnitude ($n = 13$, $r = 0.71$, $p = 0.006$), induced by noxious CRD in the TNBS-injected rats. These results suggest that the regional brain activity in the

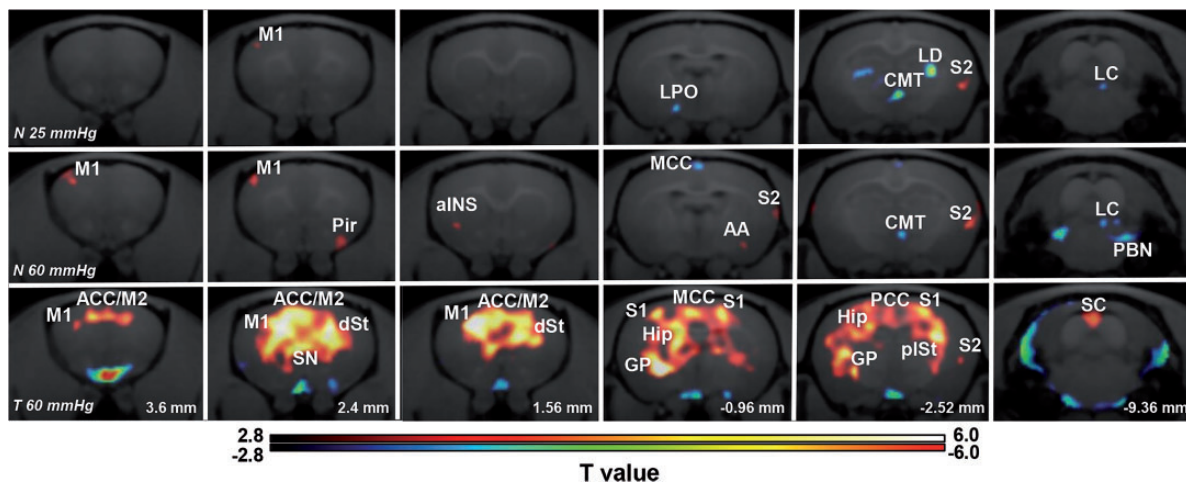


Figure 3. Brain activity in response to different colorectal distension (CRD) pressures in normal and 2,4,6-trinitrobenzene sulfonic acid (TNBS)-injected rats. Upper line (N 25 mmHg): images showing activated (red) and suppressed (blue) brain regions in normal rats that received innocuous CRD with distention pressure at 25 mmHg ($n = 9$). Middle line (N 60 mmHg): images showing activated (red) and suppressed (blue) brain regions in normal rats that received noxious CRD with distention pressure at 60 mmHg ($n = 11$). Lower line (T 60 mmHg): images showing activated (red) and suppressed (blue) brain regions in TNBS-injected rats that received innocuous CRD with distention pressure at 60 mmHg ($n = 13$). Images from each group were obtained by voxel-based statistical comparison of FDG uptake with that in the normal group with CRD pressure at 0 mmHg. The T value of 2.82 was used as the threshold corresponding to the $p < 0.005$ (uncorrected) threshold. Right sides of images indicate the right hemisphere. Numbers in the lower line indicate the level of coronal slices in rat brain atlas (Paxinos and Watson). M1/M2: primary/secondary motor cortex; S1/S2: primary/secondary somatosensory cortex; Pir: piriform cortex; AA: anterior amygdaloid area; ACC: anterior cingulate cortex; MCC: midcingulate cortex; PCC: posterior cingulate cortex; aINS: anterior insular cortex; LPO: lateral preoptic area; dSt/pLSt: dorsal/posterior lateral striatum; Hip: hippocampus; CMT: central medial thalamic nucleus; LD: laterodorsal thalamus nucleus; PBN: parabrachial nucleus; LC: locus coeruleus; SC: superior colliculus; GP: globus pallidus; SN: septal nucleus.

Table 1. Regions of greater (T value > 0) or smaller (T value < 0) activity related to the innocuous CRD in normal rats versus normal (0 mmHg) group.

Brain regions	Laterality	T value (peak)	Volume (mm ³)
Activated areas			
Primary motor cortex, M1	L	3.40	0.45
Primary somatosensory cortex, S1	R	3.38	0.36
Secondary somatosensory cortex, S2	R	4.35	1.66
Suppressed areas			
Lateral orbital cortex, LO	R	-3.73	1.10
Ventral pallidum, Vp	L	-3.94	0.65
Lateral preoptic area, LPO	L	-3.92	0.85
Laterodorsal thalamic nucleus, LD	L	-5.72	5.70
Laterodorsal thalamic nucleus, LD	R	-5.73	2.64
Medial thalamic nucleus, MD	L	-4.03	1.03
Anterodorsal thalamic nucleus, AD	R	-3.76	0.42
Central medial thalamic nucleus, CMT	L&R	-4.99	2.01
Posterior thalamic nucleus group, Po	R	-3.53	0.64
Parafascicular thalamic nucleus, PF	R	-3.69	0.35
Locus coeruleus, LC	R	-3.59	0.40
Intermediate reticular nucleus, IRt	L	-4.04	1.69
Gigantocellular reticular nucleus, Gi	R	-3.05	1.02

Note: Normal (25 mmHg) (n = 9) versus normal (0 mmHg) (n = 13). Height threshold: T = 2.82 with an extent threshold of 200 contiguous voxels, $p < 0.005$ uncorrected. L and R indicate left and right hemispheres, respectively.

Table 2. Regions of greater (T value > 0) or smaller (T value < 0) activity related to the noxious CRD in normal rats versus normal (0 mmHg) group.

Brain regions	Laterality	T value (peak)	Volume (mm ³)
Activated areas			
Primary motor cortex, M1	L	4.11	3.28
Piriform cortex, Pir	R	3.59	1.72
Anterior insular cortex, aINS	L	3.78	0.88
Lateral striatum, lSt	L	3.73	0.36
Anterior amygdaloid area, AA	R	3.49	0.44
Secondary somatosensory cortex, S2	R	4.24	5.74
Secondary auditory cortex, dorsal part, AuD	R	3.90	1.90
Cerebellar, Cb	L	3.86	1.98
Cerebellar, Cb	R	4.24	6.65
Suppressed areas			
Lateral orbital cortex, LO	L	-5.60	1.49
Lateral orbital cortex, LO	R	-3.47	0.47
Midcingulate cortex, MCC	L&R	-4.27	3.91
Central medial thalamic nucleus, CMT	L&R	-3.97	0.78
Parabrachial pigmented nucleus of the VTA, PBP	R	-3.94	0.34
Ventral hippocampus, VH	L	-3.53	0.37
Superior colliculus, SC	R	-3.75	0.71
Ventral nucleus of the lateral lemniscus, vll	L	-3.65	0.85
Parabrachial nucleus, PBN	L	-5.31	6.92
Parabrachial nucleus, PBN	R	-4.35	7.00
Locus coeruleus, LC	R	-3.70	0.72
Ventral cochlear nucleus anterior part, VCA	R	-3.98	1.88
Gigantocellular reticular nucleus, Gi	L	-3.72	0.46
Intermediate reticular nucleus, IRt	L	-4.43	1.23

Note: Normal (60 mmHg) (n = 11) versus normal (0 mmHg) (n = 13). Height threshold: T = 2.82 with an extent threshold of 200 contiguous voxels, $p < 0.005$ uncorrected. L and R indicate left and right hemispheres, respectively. VTA: ventral tegmental area.

ACC may encode nociceptive input following persistent colonic inflammation.

Subsequently, we further analyzed the functional coupling between the ACC and CMT in which the regional brain activity in the CMT was suppressed

after innocuous CRD stimulation in normal rats and disinhibited in response to noxious CRD following persistent colonic inflammation. The correlation analysis showed that the functional coupling indicated by the FDG uptake between the ACC and CMT was

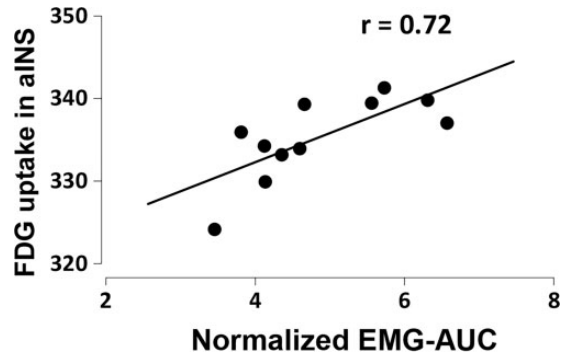


Figure 4. The correlation between FDG uptake in the anterior insular cortex and the magnitude of visceromotor response induced by noxious colorectal distension at a pressure of 60 mmHg in normal ($n = 11$, $p = 0.012$) rats. Pearson correlation analysis test. FDG: 2-deoxy-2-[^{18}F]fluoro- D -glucose; EMG-AUC: the maximal value of the area under the curve of electromyographic signals.

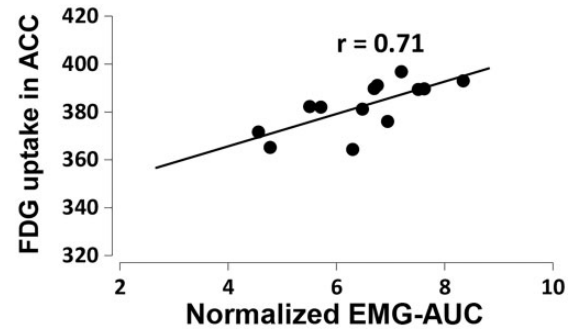


Figure 5. The correlation between FDG uptake in the ACC and the visceromotor response magnitude induced by noxious colorectal distension at a pressure of 60 mmHg in 2,4,6-trinitrobenzene sulfonic acid-injected rats ($n = 13$, $p = 0.006$). Pearson correlation analysis test. FDG: 2-deoxy-2-[^{18}F]fluoro- D -glucose; EMG-AUC: the maximal value of the area under the curve of electromyographic signals; ACC: anterior cingulate cortex.

Table 3. Regions of greater (T value > 0) or smaller (T value < 0) activity related to the noxious CRD in TNBS-injected rats versus normal (0 mmHg) group.

Brain regions	Laterality	T value (peak)	Volume (mm^3)
Activated areas			
Secondary somatosensory cortex, S2	R	3.71	0.35
Secondary auditory cortex, dorsal part, AuD	R	3.60	0.73
Entorhinal cortex, Ent	R	3.39	0.74
Cluster			281.97
Primary motor cortex, M1	L	8.34	
Anterior cingulate cortex/secondary motor cortex, ACC/M2	L&R	6.45	
Primary somatosensory cortex, S1	L	7.46	
Primary somatosensory cortex, S1	R	5.74	
Dorsal striatum, dSt	R	6.10	
Septal nucleus, SN	L&R	5.80	
Midcingulate cortex, MCC	L&R	6.39	
Posterior cingulate cortex, PCC	L&R	6.01	
Ventral striatum/globus pallidus, vSt/GP	L	11.03	
Posterior lateral striatum, plSt	R	7.46	
Hippocampus, Hip	L	6.17	
Hippocampus, Hip	L&R	5.79	
Suppressed areas			
Anterior insular cortex, aINS	L	-3.93	2.20
Cluster			407.97
Paraflocculus, PFI	L	-8.30	
Paraflocculus, PFI	R	-7.33	
Intermediate reticular nucleus, IRt	L	-8.09	
Intermediate reticular nucleus, IRt	R	-6.36	

Note: TNBS (60 mmHg) ($n = 13$) versus normal (0 mmHg) ($n = 13$). Height threshold: $T = 2.82$ with an extent threshold of 200 contiguous voxels, $p < 0.005$ uncorrected. L and R indicate left and right hemispheres, respectively.

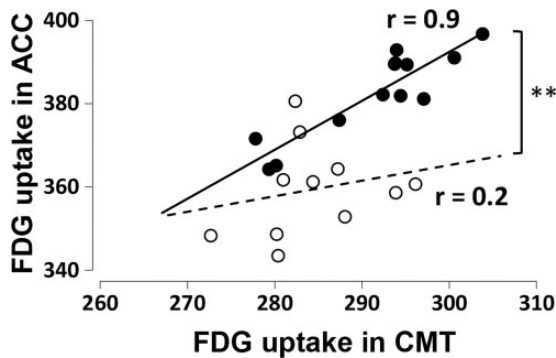


Figure 6. The functional coupling between the CMT and ACC in normal (open circle, $n = 11$, $p = 0.771$) and 2,4,6-trinitrobenzene sulfonic acid-injected (closed circle, $n = 13$, $p = 0.026 \times 10^{-3}$) rats after the induction of noxious colorectal distension at a pressure of 60 mmHg. Pearson correlation analysis test. $**p < 0.01$; Fisher's Z-transformation test. FDG: 2-deoxy-2-[18F]fluoro-D-glucose; ACC: anterior cingulate cortex; CMT: central medial thalamic nucleus.

significantly enhanced in TNBS-injected rats as compared with the normal rats after noxious CRD (Figure 6).

Discussion

In the present study, we demonstrated for the first time that the regional brain activity in the widespread brain regions was drastically changed in the IBD model rats after noxious CRD using voxel-based statistical analysis of FDG-PET imaging and found that the increased brain activity in the ACC was positively correlated with abdominal pain severity with enhanced functional coupling between the CMT following persistent colonic inflammation, suggesting that the pain matrix was shifted and the thalamocortical sensitization in the pathway from CMT to ACC might be a central mechanism of visceral hyperalgesia in IBD pathophysiology. We provide here a line of evidence that (1) colonic administration of TNBS-induced tissue damage and inflammation in the surrounding digestive tract; (2) the abdominal pain severity was quantitatively evaluated by EMG-based VMR changes in conscious condition, and the lowest VMR threshold and highest VMR magnitude were detected two days after TNBS injection; (3) distinctive brain activities were observed with innocuous and noxious CRD, respectively, except for some brain regions, such as M1 and S2, which showed similar activation even following persistent colonic inflammation; (4) noxious CRD-induced regional brain activity in the widespread regions significantly changed following persistent colonic inflammation, such as strong activation was observed in the ACC; and (5) the regional brain activity in the ACC was positively correlated with abdominal pain, and the functional coupling between

the CMT and ACC was enhanced in IBD rats. These results indicate that pain matrix was shifted following persistent colonic inflammation and the enhanced functional coupling between the CMT and ACC could play an important role in the pathophysiology of visceral hyperalgesia in IBD.

In general, pain is composed of two components: a sensory discriminatory component and an affective component. The nociceptive pathway related to the sensory discriminatory component of pain is thought to share some physiological sensory transmission circuit at least partially. Recent neuroimaging studies in healthy subjects and patients with chronic visceral pain revealed that some brain regions, such as the S1/S2 and insular cortex, seem to be similarly activated by both innocuous and noxious CRD stimulation.^{11,21–23} Meanwhile, some contradictory results have also been reported, such as the increased S2 activity was only observed by painful CRD but not by nonpainful CRD in healthy subjects.²⁴ A possible reason for the inconsistency is thought to be the different experimental design and conditions between these studies. In the present study, we clearly demonstrated that the brain activity in the M1, S2, CMT, and LC showed similar changes between innocuous and noxious CRD stimulation in normal rats. Even under persistent colonic inflammation, similar brain activity was observed in the M1 and S2, suggesting that the visceral nociceptive pathway in response to noxious CRD shares some physiological sensory transmission circuit. Indeed, the S2 region in rodent and monkey is known to receive direct afferent projections from the ventroposterior nucleus of the thalamus.^{25,26} Moreover, a magnetoencephalography study in healthy subjects also demonstrated that visceral stimuli preferentially activated the S2 rather than the S1.²⁷ These observations suggest that the regional brain activity observed in our study in the S2 contributes to visceral sensory processing evoked by both harmless and harmful stimuli.

Distinctive regional brain activities were also noted in response to the innocuous and noxious CRD, respectively. For instance, the aINS, AA, and cerebellar (Cb) regions were activated, and the PBN was suppressed after noxious CRD as compared with innocuous CRD in normal rats. Most of these brain regions have been reported to be involved in acute visceral pain perception and transmission. Neuroimaging studies in humans have demonstrated that the M1, S2, INS, and Cb are activated during noxious CRD in healthy volunteers.^{11,22,28} Activation of the amygdala in response to gastric distension was also reported in healthy volunteers²⁹ as well as in experimental animals during noxious CRD.^{30,31} Notably, the FDG uptake in the aINS, the most frequently reported brain region involved in acute visceral nociception in human and rats,^{11,19} was positively correlated with the VMR magnitude induced by noxious

CRD in the present study. Consistently, Wang et al.¹⁹ reported that visceral pain scores positively correlate with brain activity in the aINS during CRD in freely moving rats. These observations suggest that brain activity in the aINS encodes pain intensity during noxious CRD in normal rats.

Despite the distention pressure being the same (60 mmHg) between the normal and TNBS-injected rats, the activation patterns of brain activity in response to noxious CRD were drastically changed following persistent colorectal inflammation. Strong activations were seen in the ACC following persistent colonic inflammation but not in normal rats. The ACC is well known to be critically involved in the processing of an affective/emotional component of pain not only in healthy volunteers but also in patients with chronic visceral pain and thought to functionally encode nociceptive inputs.^{9,32,33} However, recent neuroimaging studies have also provided controversial evidence that brain activity in the ACC does not contribute to noxious CRD-induced visceral pain processing in healthy volunteers.^{34,35} Consistent with these reports, our study demonstrated that the regional brain activity in the ACC was increased following persistent colonic inflammation but not in the normal rats. The correlation analysis also showed that the FDG uptake in the ACC was positively correlated with VMR magnitude induced by noxious CRD in TNBS-injected rats not in the normal rats. Similarly, experimental investigations in the visceral hypersensitive model rats have reported that the ACC functionally contributes to visceral hypersensitive pain processing not nociceptive processing in normal condition. For instance, Gao et al. reported that the single neuronal activities in the ACC were significantly increased in response to noxious CRD in the rats intraperitoneally injected with chicken egg albumin as compared with the normal rats.³⁶ Moreover, chemical lesion of the ACC suppressed noxious CRD-induced VMR in the visceral hypersensitive rats but not in the normal rats.³⁷ These observations indicate that the increased brain activity in the ACC is involved in nociceptive encoding following persistent colonic inflammation.

In the present study, we also demonstrated that functional coupling between the ACC and CMT was significantly enhanced following persistent colonic inflammation under noxious CRD as compared with normal condition. Recently, the thalamocortical sensitization has been reported to be involved in the development and maintenance of various types of chronic pain. For instance, the enhanced neuronal activity in medio-dorsal (MD) thalamus and the posterior nucleus of the thalamus have been proposed to be a central mechanism of spinal cord injury pain.^{38,39} Similarly, the increased spontaneous activity in the ventral posterior (VP) thalamus was observed in the chronic neuropathic pain rats.⁴⁰

Furthermore, the central sensitization in the cortical regions have also been reported, such as potentiated thalamic transmission from MD and central lateral thalamus to ACC was observed in a visceral hypersensitive rats intraperitoneally injected with chicken egg albumin.⁴¹ In consistent with these electrophysiological experiments, enhanced resting-state functional connectivity between the pregenual ACC and thalamus within the salience network in hypersensitive irritable bowel syndrome (IBS) patients was reported in a neuroimaging study.⁴² In line with these observations, we found that functional coupling between the ACC and CMT was increased following persistent colonic inflammation. Given the fact that the CMT, a component of the intralaminar/midline thalamic complex, has strong projections into the ACC and known to be involved in affective pain processing,^{43,44} the increased brain activity in the ACC and enhanced functional coupling between the ACC and CMT suggest that the thalamocortical sensitization might be a central mechanism of visceral hyperalgesia in IBD pathophysiology. Although several early studies have reported that the CMT modulates nociceptive transmission via interact with other brain region (periaqueductal gray [PAG], VP),⁴⁵ the detailed mechanisms how the functional coupling between the CMT and ACC actually contributed to pathophysiology of visceral hyperalgesia in IBD should be explored in the near future.

Conclusions

In the present study, we demonstrated for the first time that distinctive regional brain activities were observed in response to visceral innocuous and noxious CRD in normal and IBD rats and found that the supraspinal nociceptive pathway shares some physiological sensory transmission circuit. The regional brain activity in the aINS and ACC was increased and positively correlated with noxious CRD-induced pain intensity in normal and IBD rats, respectively. Enhancement of functional coupling between the CMT and ACC was observed following the persistent colonic inflammation, suggesting that thalamocortical sensitization may play an important role in the pathophysiology of visceral hyperalgesia in IBD.

Declaration of Conflicting Interests

The author(s) declared no potential conflicts of interest with respect to the research, authorship, and/or publication of this article.

Funding

The author(s) disclosed receipt of the following financial support for the research, authorship, and/or publication of this article: This work was supported in part by a Grant-in-Aid

for Scientific Research from the Japan Society for the Promotion of Science (KAKENHI 26112003 to YC) and by A3 Foresight Program from the Japan Society for the Promotion of Science.

ORCID iD

Tianliang Huang  <https://orcid.org/0000-0002-3879-5756>

References

- Chen J, Winston JH, Fu Y, Guptarak J, Jensen KL, Shi XZ, Green TA, Sarna SK. Genesis of anxiety, depression, and ongoing abdominal discomfort in ulcerative colitis-like colon inflammation. *Am J Physiol Regul Integr Comp Physiol* 2015; 308: R18–R27.
- Lonnfors S, Vermeire S, Greco M, Hommes D, Bell C, Avedano L. IBD and health-related quality of life—discovering the true impact. *J Crohns Colitis* 2014; 8: 1281–1286.
- Bielefeldt K, Davis B, Binion DG. Pain and inflammatory bowel disease. *Inflamm Bowel Dis* 2009; 15: 778–788.
- Hillsley K, Lin JH, Stanisz A, Grundy D, Aerssens J, Peeters PJ, Moechars D, Coulie B, Stead RH. Dissecting the role of sodium currents in visceral sensory neurons in a model of chronic hyperexcitability using Nav1.8 and Nav1.9 null mice. *J Physiol* 2006; 576: 257–267.
- Jones RC III, Xu L, Gebhart GF. The mechanosensitivity of mouse colon afferent fibers and their sensitization by inflammatory mediators require transient receptor potential vanilloid 1 and acid-sensing ion channel 3. *J Neurosci* 2005; 25: 10981–10989.
- Kogure Y, Wang S, Tanaka K, Hao Y, Yamamoto S, Nishiyama N, Noguchi K, Dai Y. Elevated H₂O₂ levels in trinitrobenzene sulfate-induced colitis rats contributes to visceral hyperalgesia through interaction with the transient receptor potential ankyrin 1 cation channel. *J Gastroenterol Hepatol* 2016; 31: 1147–1153.
- Delafoy L, Gelot A, Ardid D, Eschaliere A, Bertrand C, Doherty AM, Diop L. Interactive involvement of brain derived neurotrophic factor, nerve growth factor, and calcitonin gene related peptide in colonic hypersensitivity in the rat. *Gut* 2006; 55: 940–945.
- Traub RJ, Murphy A. Colonic inflammation induces fos expression in the thoracolumbar spinal cord increasing activity in the spinoparabrachial pathway. *Pain* 2002; 95: 93–102.
- Bernstein CN, Frankenstein UN, Rawsthorne P, Pitz M, Summers R, McIntyre MC. Cortical mapping of visceral pain in patients with GI disorders using functional magnetic resonance imaging. *Am J Gastroenterol* 2002; 97: 319–327.
- Mayer EA, Berman S, Suyenobu B, Labus J, Mandelkern MA, Naliboff BD, Chang L. Differences in brain responses to visceral pain between patients with irritable bowel syndrome and ulcerative colitis. *Pain* 2005; 115: 398–409.
- Lotze M, Wietek B, Birbaumer N, Ehrhardt J, Grodd W, Enck P. Cerebral activation during anal and rectal stimulation. *Neuroimage* 2001; 14: 1027–1034.
- Zeng Y, Hu D, Yang W, Hayashinaka E, Wada Y, Watanabe Y, Zeng Q, Cui Y. A voxel-based analysis of neurobiological mechanisms in placebo analgesia in rats. *Neuroimage* 2018; 178: 602–612.
- Cui Y, Toyoda H, Sako T, Onoe K, Hayashinaka E, Wada Y, Yokoyama C, Onoe H, Kataoka Y, Watanabe Y. A voxel-based analysis of brain activity in high-order trigeminal pathway in the rat induced by cortical spreading depression. *Neuroimage* 2015; 108: 17–22.
- Morris GP, Beck PL, Herridge MS, Depew WT, Szewczuk MR, Wallace JL. Hapten-induced model of chronic inflammation and ulceration in the rat colon. *Gastroenterology* 1989; 96: 795–803.
- Ness TJ. Models of visceral nociception. *ILAR J* 1999; 40: 119–128.
- Hao Y, Nagase K, Hori K, Wang S, Kogure Y, Fukunaga K, Kashiwamura S, Yamamoto S, Nakamura S, Li J, Miwa H, Noguchi K, Dai Y. Xilei san ameliorates experimental colitis in rats by selectively degrading proinflammatory mediators and promoting mucosal repair. *Evid Based Complement Alternat Med* 2014; 2014: 1.
- Hoffmann JC, Peters K, Henschke S, Herrmann B, Pfister K, Westermann J, Zeitz M. Role of T lymphocytes in rat 2,4,6-trinitrobenzene sulphonic acid (TNBS) induced colitis: increased mortality after gamma delta T cell depletion and no effect of alpha beta T cell depletion. *Gut* 2001; 48: 489–495.
- Coutinho SV, Meller ST, Gebhart GF. Intracolonic zymosan produces visceral hyperalgesia in the rat that is mediated by spinal NMDA and non-NMDA receptors. *Brain Res* 1996; 736: 7–15.
- Wang Z, Bradesi S, Maarek JM, Lee K, Winchester WJ, Mayer EA, Holschneider DP. Regional brain activation in conscious, unrestrained rats in response to noxious visceral stimulation. *Pain* 2008; 138: 233–243.
- Drossman DA, Ringel Y, Vogt BA, Leserman J, Lin W, Smith JK, Whitehead W. Alterations of brain activity associated with resolution of emotional distress and pain in a case of severe irritable bowel syndrome. *Gastroenterology* 2003; 124: 754–761.
- Wilder-Smith CH, Schindler D, Lovblad K, Redmond SM, Nirko A. Brain functional magnetic resonance imaging of rectal pain and activation of endogenous inhibitory mechanisms in irritable bowel syndrome patient subgroups and healthy controls. *Gut* 2004; 53: 1595–1601.
- Hobday DI, Aziz Q, Thacker N, Hollander I, Jackson A, Thompson DG. A study of the cortical processing of ano-rectal sensation using functional MRI. *Brain* 2001; 124: 361–368.
- Aziz Q, Andersson JL, Valind S, Sundin A, Hamdy S, Jones AK, Foster ER, Langstrom B, Thompson DG. Identification of human brain loci processing esophageal sensation using positron emission tomography. *Gastroenterology* 1997; 113: 50–59.
- Moisset X, Bouhassira D, Denis D, Dominique G, Benoit C, Sabate JM. Anatomical connections between brain areas activated during rectal distension in healthy volunteers: a visceral pain network. *Eur J Pain* 2010; 14: 142–148.
- Stevens RT, London SM, Vania Apkarian A. Spinothalamicocortical projections to the secondary

- somatosensory cortex (SII) in squirrel monkey. *Brain Res* 1993; 631: 241–246.
26. Pierret T, Lavallée P, Deschênes M. Parallel streams for the relay of vibrissal information through thalamic barreloids. *J Neurosci* 2000; 20: 7455–7462.
 27. Schnitzler A, Volkmann J, Enck P, Frieling T, Witte OW, Freund HJ. Different cortical organization of visceral and somatic sensation in humans. *Eur J Neurosci* 1999; 11: 305–315.
 28. Kern MK, Jaradeh S, Arndorfer RC, Jesmanowicz A, Hyde J, Shaker R. Gender differences in cortical representation of rectal distension in healthy humans. *Am J Physiol Gastrointest Liver Physiol* 2001; 281: G1512–G1523.
 29. Lu CL, Wu YT, Yeh TC, Chen LF, Chang FY, Lee SD, Ho LT, Hsieh JC. Neuronal correlates of gastric pain induced by fundus distension: a 3T-fMRI study. *Neurogastroenterol Motil* 2004; 16: 575–587.
 30. Lazovic J, Wrzos HF, Yang QX, Collins CM, Smith MB, Norgren R, Matyas K, Ouyang A. Regional activation in the rat brain during visceral stimulation detected by c-fos expression and fMRI. *Neurogastroenterol Motil* 2005; 17: 548–556.
 31. Traub RJ, Silva E, Gebhart GF, Solodkin A. Noxious colorectal distention induced-c-Fos protein in limbic brain structures in the rat. *Neurosci Lett* 1996; 215: 165–168.
 32. Song GH, Venkatraman V, Ho KY, Chee MW, Yeoh KG, Wilder-Smith CH. Cortical effects of anticipation and endogenous modulation of visceral pain assessed by functional brain MRI in irritable bowel syndrome patients and healthy controls. *Pain* 2006; 126: 79–90.
 33. Mertz H, Morgan V, Tanner G, Pickens D, Price R, Shyr Y, Kessler R. Regional cerebral activation in irritable bowel syndrome and control subjects with painful and nonpainful rectal distention. *Gastroenterology* 2000; 118: 842–848.
 34. Larsson MB, Tillisch K, Craig AD, Engstrom M, Labus J, Naliboff B, Lundberg P, Strom M, Mayer EA, Walter SA. Brain responses to visceral stimuli reflect visceral sensitivity thresholds in patients with irritable bowel syndrome. *Gastroenterology* 2012; 142: 463–472.
 35. Guleria A, Karyampudi A, Singh R, Khetrapal CL, Verma A, Ghoshal UC, Kumar D. Mapping of brain activations to rectal balloon distension stimuli in male patients with irritable bowel syndrome using functional magnetic resonance imaging. *J Neurogastroenterol Motil* 2017; 23: 415–427.
 36. Gao J, Wu X, Owyang C, Li Y. Enhanced responses of the anterior cingulate cortex neurones to colonic distension in viscerally hypersensitive rats. *J Physiol* 2006; 570: 169–183.
 37. Cao Z, Wu X, Chen S, Fan J, Zhang R, Owyang C, Li Y. Anterior cingulate cortex modulates visceral pain as measured by visceromotor responses in viscerally hypersensitive rats. *Gastroenterology* 2008; 134: 535–543.
 38. Whitt JL, Masri R, Pulimood NS, Keller A. Pathological activity in mediodorsal thalamus of rats with spinal cord injury pain. *J Neurosci* 2013; 33: 3915–3926.
 39. Park A, Uddin O, Li Y, Masri R, Keller A. Pain after spinal cord injury is associated with abnormal presynaptic inhibition in the posterior nucleus of the thalamus. *J Pain* 2018; 19: 727.e1–727.e15.
 40. Patel R, Dickenson AH. Neuronal hyperexcitability in the ventral posterior thalamus of neuropathic rats: modality selective effects of pregabalin. *J Neurophysiol* 2016; 116: 159–170.
 41. Wang J, Zhang X, Cao B, Liu J, Li Y. Facilitation of synaptic transmission in the anterior cingulate cortex in viscerally hypersensitive rats. *Cereb Cortex* 2015; 25: 859–868.
 42. Icenhour A, Witt ST, Elsenbruch S, Lowen M, Engstrom M, Tillisch K, Mayer EA, Walter S. Brain functional connectivity is associated with visceral sensitivity in women with irritable bowel syndrome. *Neuroimage Clin* 2017; 15: 449–457.
 43. Vertes RP, Hoover WB, Rodriguez JJ. Projections of the central medial nucleus of the thalamus in the rat: node in cortical, striatal and limbic forebrain circuitry. *Neuroscience* 2012; 219: 120–136.
 44. Berendse HW, Groenewegen HJ. Restricted cortical termination fields of the midline and intralaminar thalamic nuclei in the rat. *Neuroscience* 1991; 42: 73–102.
 45. Weigel R, Weigel R, Krauss JK, Krauss JK. Center median-parafascicular complex and pain control. Review from a neurosurgical perspective. *Stereotact Funct Neurosurg* 2004; 82: 115–126.